

# Numerical Analysis on the Breakup of Dilute Water Spray in Gaseous Detonation

Hiroaki Watanabe<sup>1</sup>, Akiko Matsuo<sup>2</sup>, Ashwin Chinnayya<sup>3</sup>,  
Ken Matsuoka<sup>1</sup>, Akira Kawasaki<sup>1</sup>, Jiro Kasahara<sup>1</sup>

<sup>1</sup>Department of Aerospace Engineering, Nagoya University  
Furo-cho, Chikusa, Nagoya, Aichi 464-8603, Japan

<sup>2</sup>Department of Mechanical Engineering, Keio University  
3-14-1 Hiyoshi, Kohoku, Yokohama, Kanagawa 223-8522, Japan

<sup>3</sup>Institute Pprime – UPR CNRS 3346  
ENSMA, 1 avenue Clément Ader, BP 40109,  
86961 Futuroscope-Chasseneuil Cedex, France

## 1 Introduction

Under the appropriate boundary and initial conditions, a detonation can propagate at a supersonic speed relative to the reactants. In the steady ZND laminar one-dimensional model [1], the fresh gas mixture ignites by adiabatic compression by the leading shock wave, and the exothermic reaction occurs after a pool of intermediate species proliferates. Then, the flow is accelerated by the heat addition from the chemical reactions and the mean sonic plane is established, which statistically separates the detonation front from the rear. Due to the specific properties of detonation, a severe damage may occur due to high overpressure behind the detonation and detonation has to be prevented for the safety of people and installations, such as in coal mines and power plants. Therefore, the knowledge on the initiation and the mitigation of the detonation is required from the point of view of the safety engineering.

One of the potential solutions is the use of the water spray [2] and the main concern is to clarify the condition for the water spray to quench the detonation effectively. Gerstein et al. [3] have shown that water spray could quench the transition of the flame to detonation of methane-air at low pressures. Thomas et al. [4] studied the quenching of detonation by water spray of various stoichiometric mixtures diluted by nitrogen or argon. The coarser water spray with droplet diameter ranging from 500  $\mu\text{m}$  to 1100  $\mu\text{m}$  could not quench the detonation and only reduced the impulse in their experimental conditions. On the other hand, detonation was successfully quenched by the finer spray with 150-300  $\mu\text{m}$  diameter droplets. Another experimental study by Niedzielska et al. [5] pointed out a different trend for the characteristics of a water droplet curtain to quench a hydrogen-air detonation. Two water droplet curtains whose diameter was 215 and 500  $\mu\text{m}$  respectively were used. The finer spray could not extinguish the detonation, on the contrary of the coarser one. In the review by Gelfand et al. [6], the model equation for loading ratio required for quenching detonation was derived as a function of the square of droplet diameter, and the importance of the small droplet size was emphasized. Though Boeck et al. [7] did not confirm the quenching of detonation by water spray, they observed that the water droplets whose Sauter mean diameter is 13  $\mu\text{m}$  delayed the deflagration to detonation transition for the atmospheric hydrogen-air mixture and that the detonation propagation speed decreased by 3% as compared to the CJ velocity. From the aforementioned studies, the general guideline for droplet condition to quench the detonation is not achieved and the effect of water spray on detonation wave is not fully understood yet.

In order to gain some insights into the structure of gaseous detonation with water droplets (WDs) and the behavior of WDs, Watanabe et al. [8] performed two-dimensional (2-D) numerical simulations based on the previous experiment by Jarsalé et al. [9] and investigated the structure from the Favre averaged one-dimensional profiles. The velocity decrease and the change in the cellular structure by the addition of WDs were similar to the experimental results, and the structure was affected by the evaporation of WDs that was coupled with the detonation wave. Nevertheless, the numerical model used in the study by Watanabe et al. [8] did not take into account the droplet breakup that is likely to occur by the strong and unsteady shock waves behind the front producing a large amount of small droplets that enhance the two-phase interactions. Then, Watanabe et al. [10] conducted 2-D simulation with breakup modeling and compared the gaseous and WDs characteristic lengths that were quantitatively ordered and that were shown to be intimately intertwined. The induction length was shorter than the characteristic length for the end of breakup under the simulation conditions and the water vapor from the evaporation of WDs did not affect the reactivity of the gaseous mixture, which is in line with the previous finding by Jarsalé [9]. In addition, Watanabe et al. [11] analyzed the behavior of WDs and showed that the breakup occurred mainly behind the leading front. The jets and transverse waves which come from the cellular instabilities of the detonation were at the origin of the final polydispersity in the droplet diameter. The simulation results also confirmed that the non-dimensional total breakup time became longer than that estimated by the post-shock conditions due to the change in the dynamic pressure downstream of the front, in line with Ragland et al. [12] and Dabora et al. [13].

In these previous studies [8,10,11], the spray was initially monodisperse in order to allow easier analysis of the results. However, the real spray has an initial distribution in the droplet diameter, which implies that a wide range of length scales will emerge. The effect of the initial distribution of droplet diameter cannot be inferred from the previous studies. Therefore, the present study aims to clarify the behavior of the water spray with different initial size in gaseous detonation. In this report, the evolution of the distribution of droplet diameter is monitored and the outcome of the breakup process is estimated.

## 2 Mathematical modelling and numerical method

The details of the mathematical modeling and the numerical method used in the in-house code is described in previous studies [10,11,14], and the mathematical modeling and numerical method are the same. Therefore, only a brief description is presented in this section.

The detonation propagation in a water spray is related to two-phase flows of gas and droplets, which is modeled by the Eulerian–Lagrangian method. The governing equations combined with porosity for the gaseous phase are the 2-D reactive compressible Navier-Stokes equations with source terms accounting for the chemical reactions and the interactions with the droplets [10,11,14]. The chemical species are  $H_2$ ,  $O_2$ ,  $H$ ,  $O$ ,  $OH$ ,  $H_2O$ ,  $HO_2$ ,  $H_2O_2$  and  $N_2$ . The equation of state is the perfect gas law. The detailed kinetics for hydrogen is that of Hong et al. [15], with 9 species and 20 elementary reactions. The thermochemical species properties are calculated using the JANAF polynomials [16]. As for the transport properties but  $HO_2$ , a method proposed by [17] is used to estimate the gas viscosity and thermal conductivity. For  $HO_2$  species, the viscosity and thermal conductivity are calculated by the Chapman–Enskog method [18] and the Eucken method [19], respectively. The pure species diffusion coefficients are evaluated using the Chapman–Enskog method [18]. The Wilke method [20] and Wassiljewa method [21] are used to estimate the multi-component gas viscosity and thermal conductivity, respectively.

The droplet motion is modeled by the particle tracking method, equations of which are Newton's equation of motion, energy equation, and number density conservation equation. As the Biot number is much lower than unity, the temperature of the particle is considered to be uniform. The evaporation of WDs is determined by the model of Abramzon et al. [22]. The drag force is estimated by the model of Ling et al. [23] and convective heat flux is calculated using the Ranz-Marshall equation [24]. Droplet

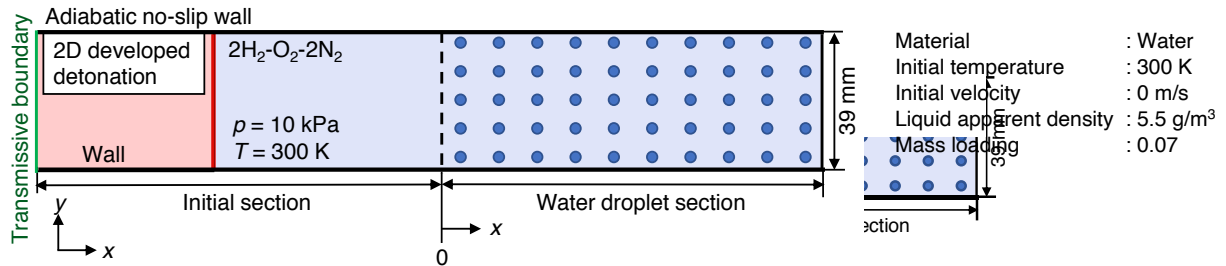


Fig. 1 Physical configuration of the simulation

breakup models can be found in [25] and the model used in this study assumes that the droplet diameter decreases linearly during the breakup process [25]. The maximum stable diameter follows from stability criterion and the total breakup time is determined by Pilch and Erdman [26].

A classical splitting method is employed to couple the hydrodynamics with the detailed chemistry and the interphase exchanges. The convective terms are discretized by fifth-order advection upstream splitting method using AUSMPW+ improved by [27] based on MWENO-Z [28] and the diffusive terms by second-order central differential schemes. The time integration method is the third-order TVD Runge-Kutta method [29], and the multi-timescale method [30] is used for efficient time integration of the chemical source terms. The droplet equations are solved with first-order methods. The porosity is then calculated using the ratio of the total volume of droplets located in the computational cell to the computational cell volume, using the particle centroid method [31]. The barycentric interpolation of [32] is used to estimate the interphase exchanges.

The validation of the present numerical model for the droplet breakup has been addressed in the previous studies [10,14], even if there is a need for further experimental work for higher initial Mach number.

### 3 Results and discussion

The physical configuration related to the numerical simulation is depicted in Fig. 1, with similar conditions as in previous studies [10,11] except for the initial droplet diameter. A fully developed gaseous detonation in the 39 mm width straight channel which propagates within a stoichiometric H<sub>2</sub>-O<sub>2</sub> premixed gas diluted with 40% N<sub>2</sub> interacts with the same premixed gas laden with WDs. The initial pressure and temperature are 10 kPa and 300 K, respectively. The WDs are uniformly distributed and the apparent density of water is 5.5 g/m<sup>3</sup>. The initial droplet diameter distribution is referred to the experimental results by Jarsalé et al. [9], where they found that the log-normal distribution fitted well with measured spray characteristics. The maximum droplet diameter in the simulation is limited to the grid cell size that has to remain greater than that of the droplet in the current numerical modeling, implying that the maximum droplet diameter in initial condition is set to 25 μm. The initial droplet diameter distribution is determined from diameter distribution in Jarsalé et al. [9] excluding the droplet over 25 μm. The droplets with different initial diameter are spatially distributed and the probability density function (pdf) for the initial droplet diameter is shown in Fig. 2. The arithmetic mean diameter and the Sauter mean diameter are 10.3 μm and 14.9 μm, respectively. The wall is an adiabatic no-slip wall, and the left boundary is an outflow. The half reaction length (*hrl*) is 1696 μm. The minimum grid width is 50 μm and the resolution is about 34 pts/*hrl*. The non-dimensional activation energy for this

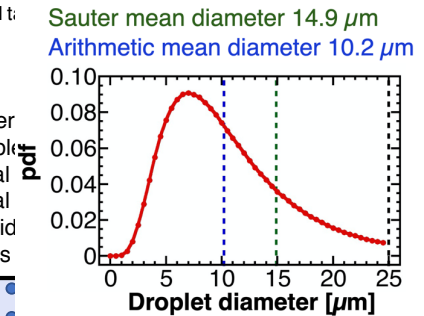


Fig. 2 Pdf of initial droplet diameter

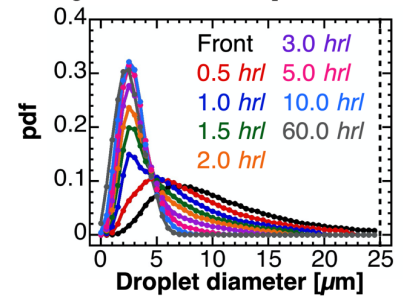


Fig. 3 Pdf of droplet diameter for several distances from the shock front

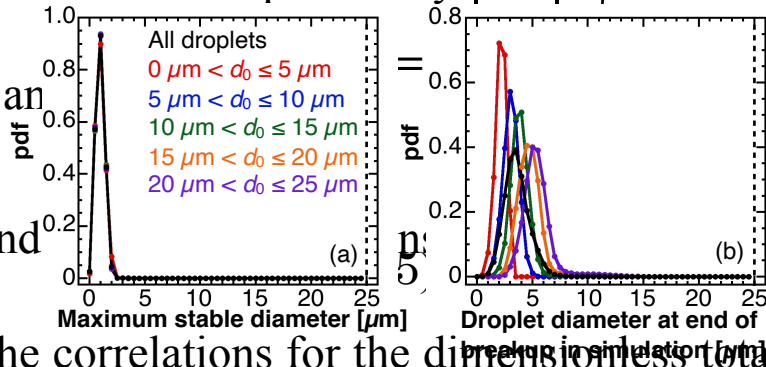


Fig. 4 (a) pdf of maximum stable diameter determined from post-shock values in simulation, (b) pdf of droplet diameter at end of breakup in simulation

mixture in the present reaction model is 5.5, which can be classified as a weakly unstable mixture according to the stability analysis. The role of turbulent burning in weakly unstable mixture is not important, contrary to highly unstable mixture with irregular cellular structure. The present phenomena can be well resolved with the present grid resolution.

The recycling block method is used. The length of the computational domain with minimum grid size is set to 120 mm in the present study, length of which encompasses the mean leading shock front and the mean sonic plane. In the present computations, the detonation has propagated over a distance of 2000 mm. Then the 2-D data from 500 mm to 2000 mm after the first contact with WDs enable to evaluate the mean and statistical values.

The Probability Density Function (pdf) of the droplet diameter and the initial droplet diameter are shown in Fig. 3 for several distances from the shock front in order to evaluate their evolution. The pdf became narrower and its peak value was higher toward the end of the breakup process (Fig. 3), which meant that the breakup played a role in regularizing the droplet diameter. Nevertheless, even if it could be expected from the results in [11,14] from an initial monodisperse spray that the jets and transverse waves would enlarge the initial pdf, the polydispersity of the resulting droplet diameter remained limited here. After the breakup process, the shapes of the pdf were similar and the droplet diameter then gradually decreased by the evaporation.

The maximum stable diameter  $d_{st} = We_c \sigma / (\rho_g |\mathbf{u}_r|^2)$  is independent of the initial droplet diameter and depends only on the dynamic pressure, the gas density  $\rho_g$  and the relative velocity between phases  $\mathbf{u}_r$ , under the assumption that the surface tension and the critical Weber number  $We_c$  are constant. Indeed, the shape of the pdf for the maximum stable diameter was the same regardless of the initial droplet diameter, its distribution coming from the fluctuations in the gas quantities behind the front due to the cellular instabilities (Fig. 4(a)). On the other hand, closer inspection of the droplet diameter at the end of the breakup in the simulation showed that it was affected to some extent by the initial droplet diameter (Fig. 4(b)). As the initial droplet diameter was smaller, the droplet diameter at the end of breakup was smaller and the final distribution at the end of breakup was narrower as the initial droplet diameter was smaller. This dependence of the final droplet diameter on the initial droplet diameter came from the change in the dynamic pressure during the breakup process [11,14] (Fig. 5), due to gas expansion and momentum exchange. Indeed, Gelfand [33] pointed out that the duration of supercritical conditions and the time-dependent profiles affected the evolution and outcome of droplet breakup. The time scale for the end of breakup ( $\tau \propto d/|\mathbf{u}_r| \cdot (\rho_l/\rho_g)^{1/2}$ ) increased as the droplet was initially larger. Thus, the larger droplets experienced lower dynamic pressures during the characteristic time scale of the breakup process (Fig. 5), meaning that the corresponding stable value was also increasing (Fig. 4(b)). The profile of pdf in Fig. 4(b) was also wider as the larger droplets would experience much further dynamic events than the smaller ones.

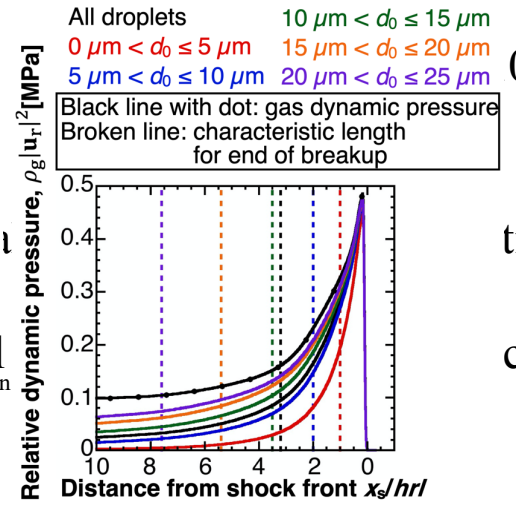


Fig. 5 Averaged 1-D profile for the relative dynamic pressure. The vertical lines represent the location of the end of breakup for the different classes

The outcome of the breakup process was evaluated in terms of the non-dimensional total breakup time in Fig. 6. As mentioned above, the dynamic pressure changed during the breakup process (Fig. 5) and this generally caused the longer non-dimensional breakup time and the larger droplet diameter at the end of breakup than those estimated based only on the post-shock conditions (Fig. 6(a)). The trend of longer non-dimensional total breakup time than that for the post-shock condition is in line with the experimental results of Ragland et al. [12] and Dabora et al. [13]. Dabora et al. [13] suggested to use the average dynamic pressure for a better estimation of the actual breakup time in detonation from the idea that “*drop in a detonation is subjected to a varying dynamic pressure due to the continuously changing conditions behind the front*”. The estimation based on the average relative dynamic pressure between the front and the point where the breakup finished was greatly improved as compared to that using the post shock conditions (Figs. 6(a)(b)). The use of the averaged dynamic pressure gave 1.05 as an average value for the ratio of the total breakup time in simulation to the estimation and narrowed the profiles around the simulated value (Fig. 6(c)).

#### 4 Conclusions

The behavior of the polydisperse spray in gaseous detonation were numerically analyzed using the 2-D numerical simulation, based on an Eulerian-Lagrangian method. The distribution in the droplet diameter was regularized by the breakup process. The polydispersity in the final droplet diameter at the end of the breakup process came from the cellular instabilities (fluctuations in the gas quantities at the shock front) and the degree of the change in the dynamic pressure during the breakup process, which was affected by the initial droplet diameter. In addition, the outcome of the breakup process was underestimated and deviated from the estimation based on the post-shock conditions. Indeed, the average relative dynamic pressure between the front and the point where the breakup is completed should be used for the better estimation for the total breakup time as Dabora et al. [13] suggested. The use of the averaged dynamic pressure gave 1.05 as an average value for the ratio of the total breakup time in simulations to the estimated values whereas the average value for this ratio based on the post-shock conditions was 2.20.

#### Acknowledgment

This research is subsidized by JSPS KAKENHI Grant Number JP19J12758, 20K22391, 21K14094. This work is partially supported by “Joint Usage/Research Center for Interdisciplinary Large-scale Information Infrastructures”

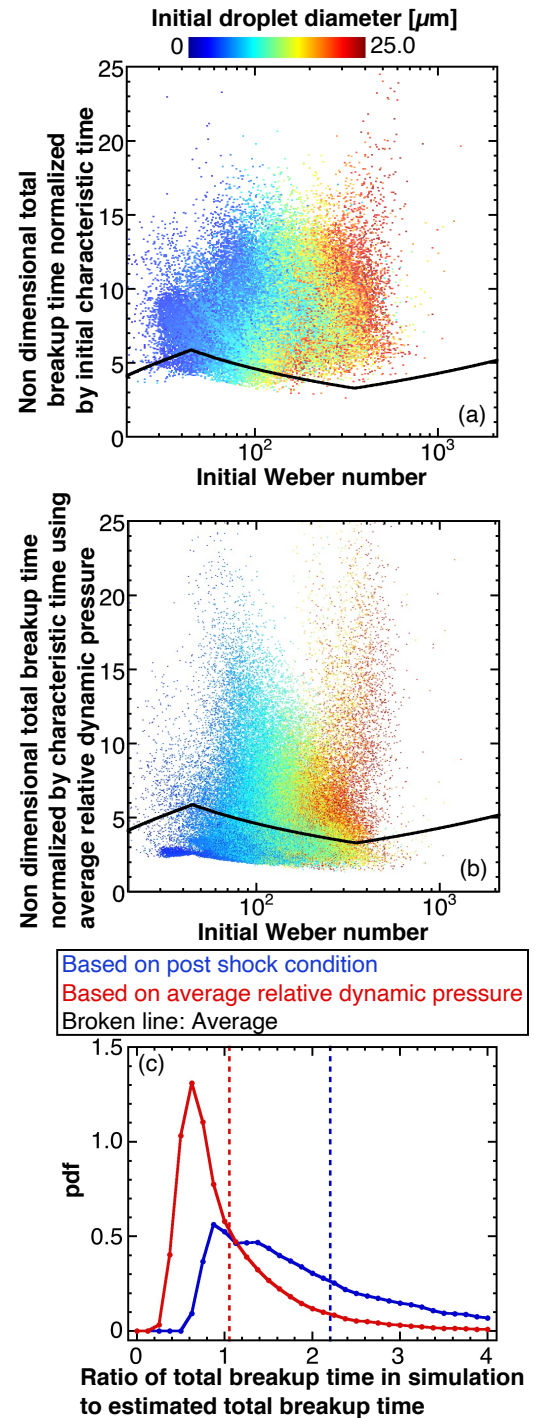


Fig. 6 Outcome of breakup process. (a) scatter plot between non-dimensional total breakup time, normalized by initial characteristic time estimated from post shock condition and initial Weber number, (b) scatter plot between non-dimensional total breakup time, normalized by initial characteristic time estimated from the average relative dynamic pressure and initial Weber number, (c) pdf of the ratio of total breakup to estimated total breakup time using average dynamic pressure. Black line in (a)(b) refers to Pilch and Erdman [26]

and “High Performance Computing Infrastructure” in Japan (Project ID: jh170040, jh180030 and hp170039). Some of the simulated results in this research were obtained using supercomputing resources at Cyberscience Center, Tohoku University. An Academic visit of Ashwin Chinnayya to Keio University as Guest Professor (Global) was made possible through a funding for top Global University Project in the Keio University. This work was supported by the CPER FEDER Project of Région Nouvelle Aquitaine and pertains to the French government program "Investissements d'Avenir" (EUR INTREE, reference ANR-18-EURE-0010)

## References

- [1] J. H. S. Lee, *The detonation phenomenon*, Cambridge University Press, 2008.
- [2] D. Allason, C. H. Mediana, D. M. Johnson, A. Pékalski, A. Dutertre, D. Mansfield, Explosion safety gap reduction with water curtain, *J. Loss Prevent. Proc. Ind.* 61 (2019) 66-81.
- [3] M. Gerstein, E. R. Carlson, F. U. Hill, Natural gas-air explosion at reduced pressure detonation velocities and pressure, *Ind. Eng. Chem. Res.* 46 (1954) 2558-2562.
- [4] G. O. Thomas, M. J. Edwards, D.H. Edwards, Studies of detonation quenching by water spray, *Combust. Sci. Technol.* 71 (1990) 233-245.
- [5] U. Niedzeilska, L. J. Kapusta, B. Savard, A. Teodorczyk, Influence of water droplets on propagating detonations, *J. Loss Prevent. Proc. Ind.* 50 (2017) 229-236.
- [6] B. E. Gelfand, S. M. Frolov, M. A. Nettleton, Gaseous detonation – a selective review, *Prog. Energy Combust. Sci.* 17 (1991) 327-371.
- [7] L. R. Boeck, A. Kink, D. Oezdin, J. Hasslberger, T. Sattelmayer, Influence of water mist on flame acceleration, DDT, and detonation in H<sub>2</sub>-air mixture, *Int. J. Hydro. Energy* 40 (2015) 6995-7004.
- [8] H. Watanabe, A. Matsuo, K. Matsuoka, A. Kawasaki, J. Kasahara, Numerical investigation on propagation behavior of gaseous detonation in water spray, *Proc. Combust. Inst.* 37 (2019) 3617-3626.
- [9] G. Jarsalé, F. Virot, A. Chinnayya, Ethylene-air detonation in water spray, *Shock Waves* 26 (2016) 561-572.
- [10] H. Watanabe, A. Matsuo, A. Chinnayya, K. Matsuoka, A. Kawasaki, J. Kasahara, Numerical analysis of the mean structure of gaseous detonation with dilute water spray, *J. Fluid Mech.* 887 (2020) A4.
- [11] H. Watanabe, A. Matsuo, A. Chinnayya, K. Matsuoka, A. Kawasaki, J. Kasahara, Numerical analysis on behavior of dilute water droplets in detonation, *Proc. Combust. Inst.* 38 (2021) 3709-3716.
- [12] K. W. Ragland, E. K. Dabora, J. A. Nicholls, Observed structure of spray detonations, *Phys. Fluids* 11 (1968) 2377-2388.
- [13] E. K. Dabora, K. W. Ragland, J. A. Nicholls, Drop-size effect in spray detonations, *Proc. Combust. Inst.* 12 (1969) 19-26.
- [14] H. Watanabe, Gaseous detonation with dilute water spray in a two-dimensional straight channel: analysis based on numerical simulation, PhD thesis, Keio University, Yokohama, Japan, 2020.
- [15] Z. Hong, D. F. Davidson, R. K. Hanson, An improved H<sub>2</sub>/O<sub>2</sub> mechanism based on recent shock tube/laser absorption measurements, *Combust. Flame* 158 (2011) 633-644.
- [16] B. J. McBride, S. Gordon, M. A. Reno, Coefficients for Calculating Thermodynamic and Transport Properties of Individual Species, NASA Technical Memorandum 4513, (1993).
- [17] S. Gordon, B. J. McBride, F. J. Zeleznik, Computer Program for Calculation of Complex Chemical Equilibrium Compositions and Applications Supplement I – Transport Properties, NASA Technical Memorandum 86885, (1984).
- [18] S. Chapman, T. G. Cowling, *The Mathematical Theory of Non-uniform Gases* third edition, Cambridge University Press, U.K., 1991.
- [19] B. E. Poling, J. M. Prausnitz, J. P. O'Connell, *The properties of gases and liquids*, 5<sup>th</sup> edition, McGraw-Hill Education, U.S., 2001.
- [20] C. R. Wilke, A Viscosity Equation for Gas Mixture, *J. Chem. Phys.* 18 (1950) 517-519.
- [21] A. Wassiljewa, Heat Conduction in Gas Mixture, *Physicalische zeitschrift* 5 (1904) 737-742.
- [22] B. Abramzon, W. A. Sirignano, Droplet vaporization model for spray combustion calculations, *Int. J. Heat Mass Trans.* 32 (1989) 1605-1618.
- [23] Y. Ling, J. L. Wagner, S. J. Beresh, S. P. Kearney, S. Balachandar, Interaction of a planar shock wave with a dense particle curtain: Modeling and experiments, *Phys. Fluids* 24 (2012) 113301.
- [24] W. E. Ranz, JR. W. R. Marshall, Evaporation from drops Part I, *Chem. Eng. Prog.* 48 (1952) 141-146.
- [25] A. Chauvin, E. Daniel, A. Chinnayya, J. Massoni, G. Jourdan, Shock waves in sprays: numerical study of secondary atomization and experimental comparison, *Shock Waves* 26 (2016) 403-415.
- [26] M. Pilch, C. A. Erdman, Use of breakup time data and velocity history data to predict the maximum size of stable fragments for acceleration-induced breakup of a liquid drop, *Int. J. Multiph. Flow* 13 (1987) 741-757.
- [27] K. H. Kim, C. Kim, O. Rho, Methods for the Accurate Computations of Hypersonic Flow I. AUSMPW+ Scheme, *J. Comput. Phys.* 174 (2001) 38-80.
- [28] F. Hu, R. Wang, X. Chen, A modified fifth-order WENOZ method for hyperbolic conservation laws, *J. Comput. Appl. Math.* 303 (2016) 56-68.
- [29] S. Gottlieb, C. Shu, E. Tadmor, Strong stability-preserving high-order time discretization method, *SIAM Rev.* 43 (2001) 89-112.
- [30] X. Gou, W. Sun, Z. Chen, Y. Ju, A dynamic multi-timescale method for combustion modeling with detailed and reduced chemical kinetic mechanisms, *Combust. Flame* 157 (2010) 1111-1121.
- [31] R. Sun, H. Xiao, Diffusion-based coarse graining in hybrid continuum-discrete solvers: Theoretical formulation and a priori tests, *Int. J. Multiph. Flow* 77 (2015) 142-157.
- [32] K. Shimura, A. Matsuo, Two-dimensional CFD-DEM simulation of vertical shock wave-induced dust lifting processes, *Shock Waves* 28 (2018) 1285-1297.
- [33] B. E. Gelfand, Droplet breakup phenomena in flows with velocity lag, *Prog. Energy Combust. Sci.* 22 (1996) 201-265.